Article

Facies and Origin of Tufa Deposits from the Gostilje River Basin and the Sopotnica River Basin (SW Serbia)

Natalija Batoćanin [1,*], Wojciech Wróblewski [2], Ivana Carević [1], Uroš Durlević [1], Violeta Gajić [3] and Aleksandar Valjarević [1]

1   Faculty of Geography, University of Belgrade, Studentski trg 3/3, 11000 Belgrade, Serbia
2   Institute of Geological Sciences, Jagiellonian University, Gronostajowa 3a, 30-387 Krakow, Poland
3   Faculty of Mining and Geology, University of Belgrade, Đušina 7, 11000 Belgrade, Serbia
*   Correspondence: natalija.batocanin@gef.bg.ac.rs

Abstract: Tufa accumulations from the Gostilje River Basin and the Sopotnica River Basin in SW Serbia are represented by both active and fossil tufa precipitates. The aim of this study is to distinguish and describe different tufa facies and to determine the environmental conditions, based on stable isotope data. We also compare our analysis with other tufa deposits in Europe. Four facies are distinguished: moss tufa, algal tufa, stromatolitic laminated tufa, and phytoclastic tufa. The dominant constituent of all tufa samples is low Mg-calcite, whereas the presence of sylvite is noted in two samples from the Gostilje River Basin. The $\delta^{18}O$ values range from $-9.07‰$ to $-10.79‰$ (mean value: $-9.81‰$), while the $\delta^{13}C$ values range from $-6.50‰$ to $-10.34‰$ (mean values $-9.01‰$). The stable isotope values ($\delta^{13}C$ and $\delta^{18}O$) indicate that these tufa deposits were precipitated from cold, ambient water supported by CO_2 of an atmospheric origin. We emphasize that this is the first data about stable isotope analyses of tufa deposits from Serbia.

Keywords: tufa; facies; stable isotopes; Sopotnica River Basin; Gostilje River Basin; Serbia

1. Introduction

Tufa is a result of calcium carbonate precipitation under cool, ambient temperature in freshwater saturated in CaCO3. Therefore, tufa is found in fluvial, lacustrine, and palustrine environments [1]. Tufas are highly porous, poorly bedded [2], and composed of calcite precipitated from calcium bicarbonate water derived from the dissolution of carbonate rocks [3]. Tufa can be deposited both at springs and downstream at rapids or waterfalls, depending on the rate of CO_2 release. The first case occurs when dissolved CO_2 in groundwater, in equilibrium with soil CO_2 partial pressure, outgasses due to the lower partial pressure of CO_2 in the atmosphere. In the second case, there is a sharp increase in the outgassing rate due to the increased surface area between water and air caused by turbulence [4]. Tufa deposits usually contain abundant remains of micro- and macrophytes, invertebrates, and bacteria [5–8] and are characterized by a low or medium deposition rate (up to a few mm per year). Tufa deposition is related to specific, clearly defined geological, geomorphological, and environmental conditions, which, together, represent synonyms for "healthy" and preserved natural environments [9]. The distribution of tufa deposits depends on the availability of meteoric water and on local and climatic conditions. Since tufa often occurs at waterfalls, its distribution is also related to the microclimate in their immediate vicinity, which is characterized by cooler temperatures and higher humidity than in the surrounding area. Tufa deposits are a useful tool for deciphering long-term climatic changes during the Quaternary period, as they can be accurately dated using a variety of dating techniques [10]. The potential of fluvial tufa deposits as a valuable archive for paleoenvironmental and paleoclimate reconstructions has been investigated in several studies that focused on tufa oxygen and carbon isotopes and geochemical proxies [4,11–20].

The most used carbonate in paleoenvironmental reconstructions is calcite, as its precipitation is accompanied by the fractionation of stable carbon and oxygen isotopes [21]. A large number of tufa deposits is recorded on the territory of Serbia, mainly in eastern Serbia, but also in western Serbia, within the Dinaric Karst. They are located south of the Danube River and Sava River, usually at altitudes higher than 500 m.a.s.l. The bibliography of tufa accumulations in Serbia is insufficient. Most of the papers have been published in local languages and journals and are, therefore, not accessible to a wide geological community. In recent decades, more attention has been paid to individual smaller deposits in the context of environmental protection and geological heritage. Nevertheless, many authors have dealt with similar tufa deposits in the region [17,20,22–30]. The importance of tufa deposits is unambiguous. As it precipitates relatively fast, in specific conditions, it can serve as an applicable tool for the comparison of environmental conditions and regional correlations with similar deposits. Tufa deposits in Serbia were important in medieval time, as they were frequently used as a building material. However, nowadays, most of these deposits are under protection and exploitation is forbidden. In this work, tufa deposits from two sites were studied—tufa of the Sopotnica River Basin (further: SRB) and tufa of the Gostilje River Basin (further: GRB). Both sites include active and fossil tufa accumulations. The main goal of this study is to distinguish and describe different tufa facies and to determine environmental conditions based on stable isotope analysis. We also give a comparison with other tufa deposits in the region, as well as in Europe.

2. Study Sites

Two sites of active and fossil tufa accumulations were selected for this study. Tufa accumulations of the Sopotnica River appear in the village of the same name at the western slopes of the mountain Jadovnik, at about 15 km from the city of Prijepolje in southwestern Serbia. Tufa accumulations of the Gostiljska River are located approximately 25 km from the center of the Zlatibor Mountain. The geographical position of both sites is given in Figure 1.

SRB and GRB are located within the NW–SE trending Dinaridic ophiolite belt (DOB), which represents a remnant of an ocean-type basin. It comprises two essential components: Mélange, also known as the Dinaride olistostrome; and the ultramafic bodies, also known as the Dinaride ophiolites [31,32].

In Serbia, about 9% of the territory is made of carbonate rocks [33], which cover mostly the Western (Dinaric Karst) and Eastern (Carpatho-Balkanides) part of Serbia. Both sites of the SRB and GRB are part of the Dinaric Karst, which is the largest continuous karstland in Europe, covering approximately 60,000 km^2 [34]. The whole area is fed by karstic springs of Mesozoic limestones, which commonly exceed several hundred meters in thickness.

Tufa accumulations of the Sopotnica River appear in the village of the same name on the western slopes of the mountain Jadovnik, about 15 km from the city of Prijepolje in southwestern Serbia. The Sopotnica River is a short tributary of the Lim River, having a source in the Middle Triassic limestones in the village of the same name. At the contact of limestones and serpentinites, the underground river emerges and continues its flow as the Sopotnica River. The whole Jadovnik Mountain is intensively karstified and lacks of surface flows [9]. The Sopotnica River drains most of the mountain.

Tufa accumulations of the Gostiljska River are located approximately 25 km from the center of the Zlatibor Mountain, where twelve thermal springs occur in the Triassic limestones. Ten of them, including Gostilje, appear at the edge of the Zlatibor ultramafic massif. The Gostiljska River is a short tributary of the Katušnica River. The spring of the Gostiljska River is in the Triassic limestones, which cover an area of about 900 km^2 [31,35].
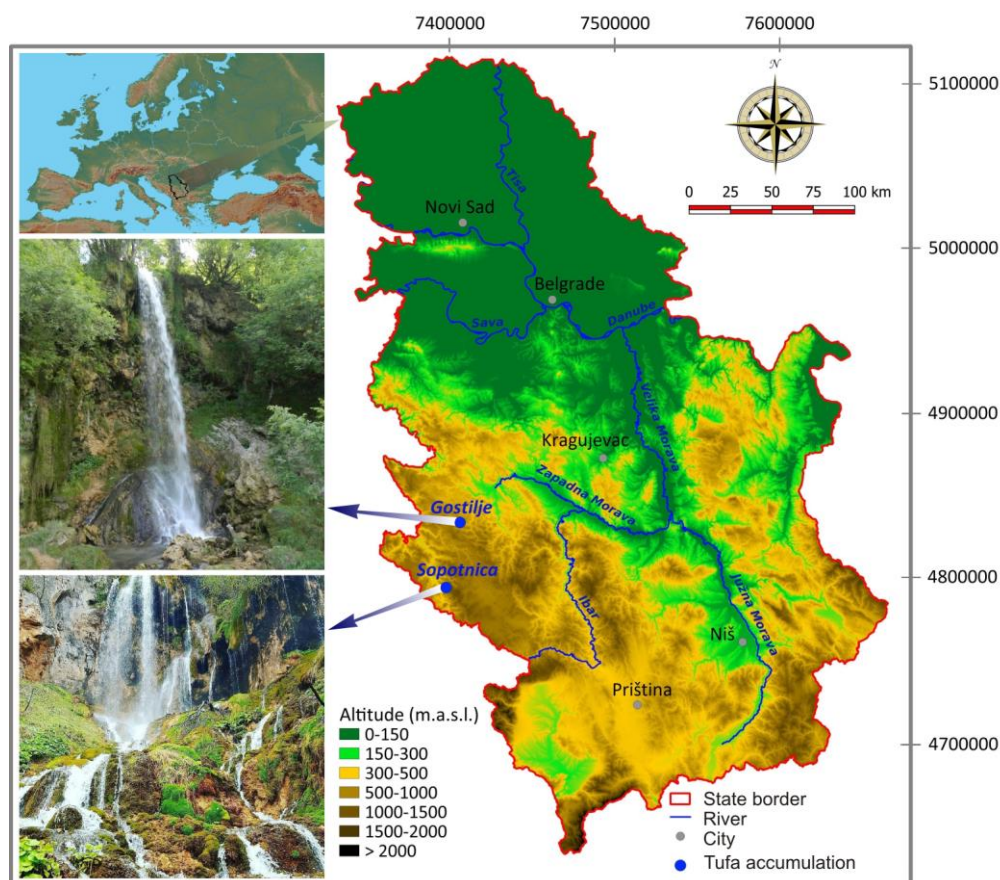
Figure 1. Geographical position of the studied sites.

3. Materials and Methods

Field work and sample selection was performed during the autumn months of 2020. A total of 59 tufa samples were collected at two locations—in the GRB and in the SRB. Tufa samples were collected from: active waterfalls, barrages, pools (recent tufa), inactive waterfalls, and fossil calcareous tufa. Facies are mainly distinguished based on field observations and confirmed afterward by detailed analyzes in thin sections. All samples were cleaned of weathered surfaces, before preparing thin sections, and then optically analyzed using a petrographic polarized microscope for transmitted light (Leica DMLSP), which was connected to a Leica DFC290 HD camera via the LAS V4.1 application. The mineralogical compositions of the twelve samples were determined by X-ray powder diffraction (XRD). Fifteen representative tufa samples were selected and examined using a JEOL JSM-6610LV scanning electron microscope connected to an X-Max energy dispersion spectrometer. Samples were covered with carbon using a BALTEC-SCD-005 Sputter coating device. Results were recorded under high vacuum conditions with an accelerating voltage of 20 kV and a beam current of 0.5–1.8 nA. All the above analyses were performed at the Department of Mineralogy, Crystallography, Petrology and Geochemistry, Faculty of Mining and Geology, University of Belgrade.

Stable isotope (oxygen and carbon) signatures in tufa have been used to clarify important climatic and environmental conditions in their formation [3,12,36–42]. In general, oxygen isotopes are indicators for paleotemperature, while carbon isotopes can point to a source of CO_2. A set of eight samples (four samples from SRB, as well as four samples from GRB) was selected for stable isotope analyzes. Stable oxygen and carbon isotope values ($\delta^{13}C$ and $\delta^{18}O$) of the carbonates were measured at the Jožef Stefan Institute in Ljubljana, Slovenia. The measurements were calibrated on the VPDB scale with the reference materials IAEA-CO8 and NBS-19. The measurements' precision was better than 0.1‰ for both the O and C values.

4. Results

4.1. Tufa Morphology and Petrology

Both localities are characterized by both active and fossil tufa precipitation, due to the changed direction of the river flow. Tufa is actively forming throughout the entire river flow at: waterfalls, cascades, and at the river bottom. Finally, deposition of the phytoclastic material led to the formation of dams and barrages, which locally surround pools. Dams and barrages are developed transverse to the watercourse. At those dams, barrages, and pools, there is also active tufa precipitation. The size of the barrages ranges from 10 cm to a few decimeters in height, and they are usually irregular or tongue shaped. They occur as single or as several piled-up barrages (Figure 2e).
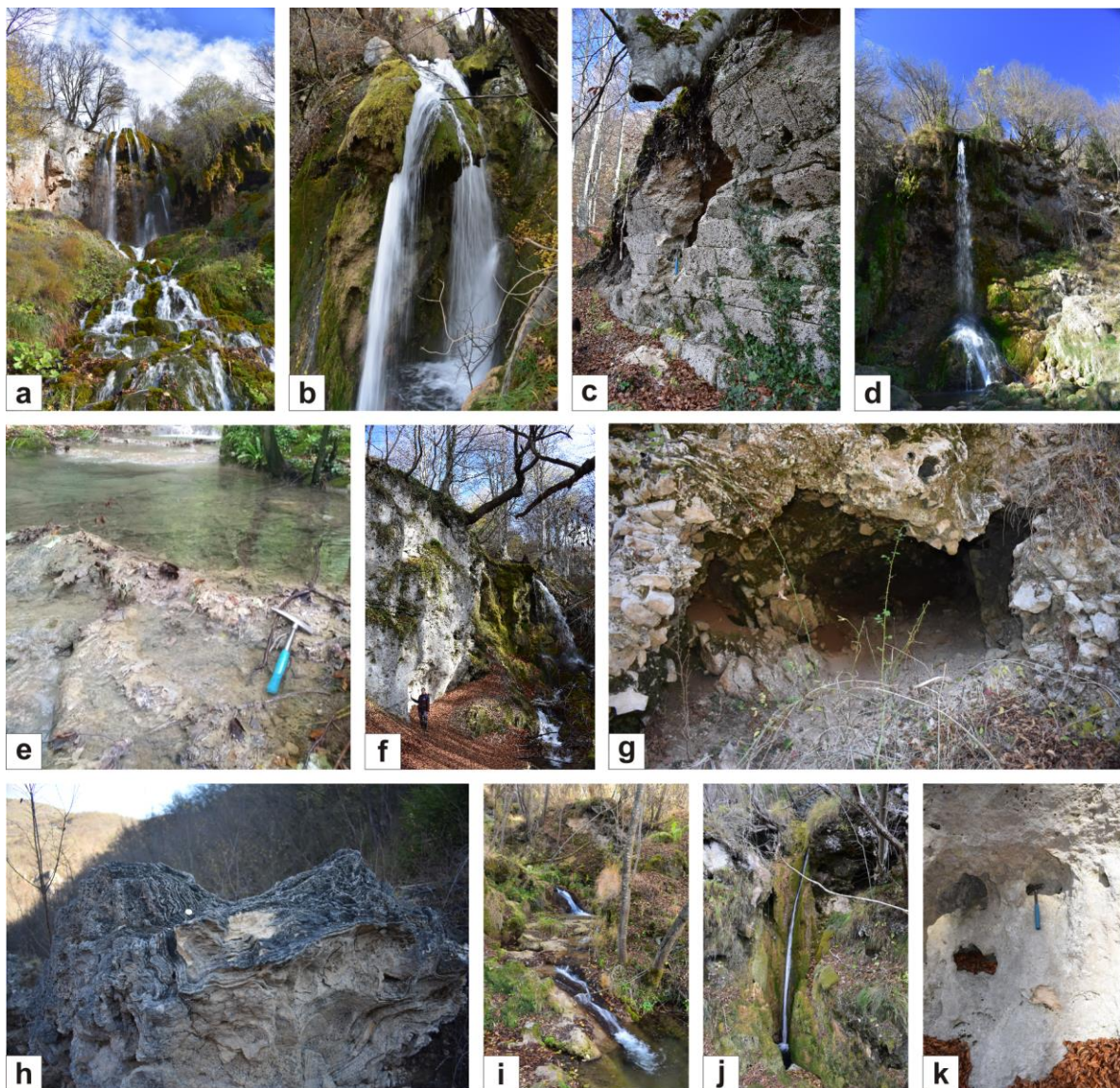

Figure 2. (**a**) The tallest, multi-step waterfall at the River Sopotnica with active tufa precipitation; (**b**) Curtain-type waterfall at the River Sopotnica; (**c**) Fossil tufa, with visible traces of exploitation; (**d**) The main waterfall at Gostiljska River with active tufa precipitation; (**e**) Several tufa barrages surrounding swallow pools; (**f**) Fossil tufa outcrop; (**g**) Limestone fragments mixed with tufa debris; (**h**) Stromatolitic laminated fossil tufa; (**i**) Algae occupying the river bottom; (**j**) "Dry" waterfall; (**k**) Fossil tufa.

The pools vary in length and width from a few decimeters to 3 m, and water depth is around a few decimeters, up to one meter maximum. Tufa outcrops differ in size; sometimes they reach 12 m in height (Figure 2f). Outcrops are well preserved, and their lateral extension varies, but it usually is less than 100 m. Fossil tufa is white, very hard, compact (Figure 2k), and contains less organic matter. On the other side, recent tufa is brownish, more porous, and has many plants' remains. The thickness of tufa bodies is variable, sometimes reaching 20 m. Older, allochthonous tufa is sporadically present as debris. In some places, tufa debris is mixed with fragmented limestones (Figure 2g). On the riverbanks, fossil tufa sometimes displays well-developed lamination (Figure 2h).

Tufa accumulations of the Sopotnica River appear in the village of the same name at the western slopes of the mountain Jadovnik, at 1100 m.a.s.l. Although it flows shortly, at about 3.5 km, the Sopotnica River creates a series of waterfalls all the way down before its confluence with the Lim River, due to having constant stream throughout the year. The tallest waterfall is 25 m in height (Figure 2a), and, generally, it is a multi-step waterfall [43]. Locally, the waterfalls display features of both a segmented and curtain type (Figure 2b). The other waterfalls are on average 19–23 m in height. Some of the smaller waterfalls are active only during spring, while they are dry during other months (Figure 2j). The deposition of tufa starts beneath the limestone cliff Podstijenje at 1120 m.a.s.l. and continues down to 850 m.a.s.l., i.e., within 270 m in vertical directions and, for some, 500 m over mélange rocks. The deposition of tufa was disrupted at the middle of the river flow, due to exploitation (Figure 2c).

Tufa accumulations of the Gostiljska River are located approximately 25 km from the center of Zlatibor Mountain, at 867 m.a.s.l. Despite its short flow (about 2 km), the Gostiljska River creates tufa accumulations along the whole flow, as well as numerous waterfalls and small cascades. The biggest of them is 22 m high and it is created just before the end of the river flow, before its confluence with the Katušnica River (Figure 2d). Water drops abruptly from a 22 m high limestone cliff, forming further in the course of river, a several smaller tiered waterfalls and rapids yet to its confluence with the Katušnica River. Those waterfalls and rapids are always covered with hanging stems, mosses, and grass.

According to the results obtained by XRD investigations, the dominant constituent of all tufa samples is low-Mg calcite (LMC). The terrigenous component was too low to be identified with XRD, but SEM analysis confirmed the presence of sand- and silt-sized detrital quartz, as well as sylvite. The former occurs in isometric, oval-shaped grains, and its presence is noted in numerous samples and in all facies except the stromatolitic laminated tufa. The latter was found only in two samples of algal tufa from the Gostilje River basin. Even macroscopically tufa samples are very different, and four facies could be distinguished, ordered by their abundance: moss tufa, phytoclastic tufa, algal tufa, and stromatolitic laminated tufa. In general, micrite is the most abundant constituent in all facies, except for the stromatolitic laminated tufa, where sparite is dominant.

4.2. Tufa Facies

Four tufa facies are recognized herein. They range from moss, algal, stromatolitic laminated, and phytoclastic tufa facies.

Moss tufa is the most common facies at studied localities. Mosses are widespread, especially in the SRB, where they usually occur at the steep sides and waterfalls (Figure 2a,b). The moss filaments are generally randomly oriented (Figure 3b).

Moss tufa consists dominantly of micrite, but sparite and microsparite are also observed (Figure 4c). The size of the individual crystals varies, but, in general, they are less than 0.1 mm and, most commonly, isometric or elongated. Oval-shaped or irregular voids, which are usually empty, are the most abundant in moss tufa. Further magnification showed that moss tufa usually consists of rhombohedron calcite crystals (Figure 5c), as well as dagger-like, elongated crystals with sharp edges (Figure 5d).
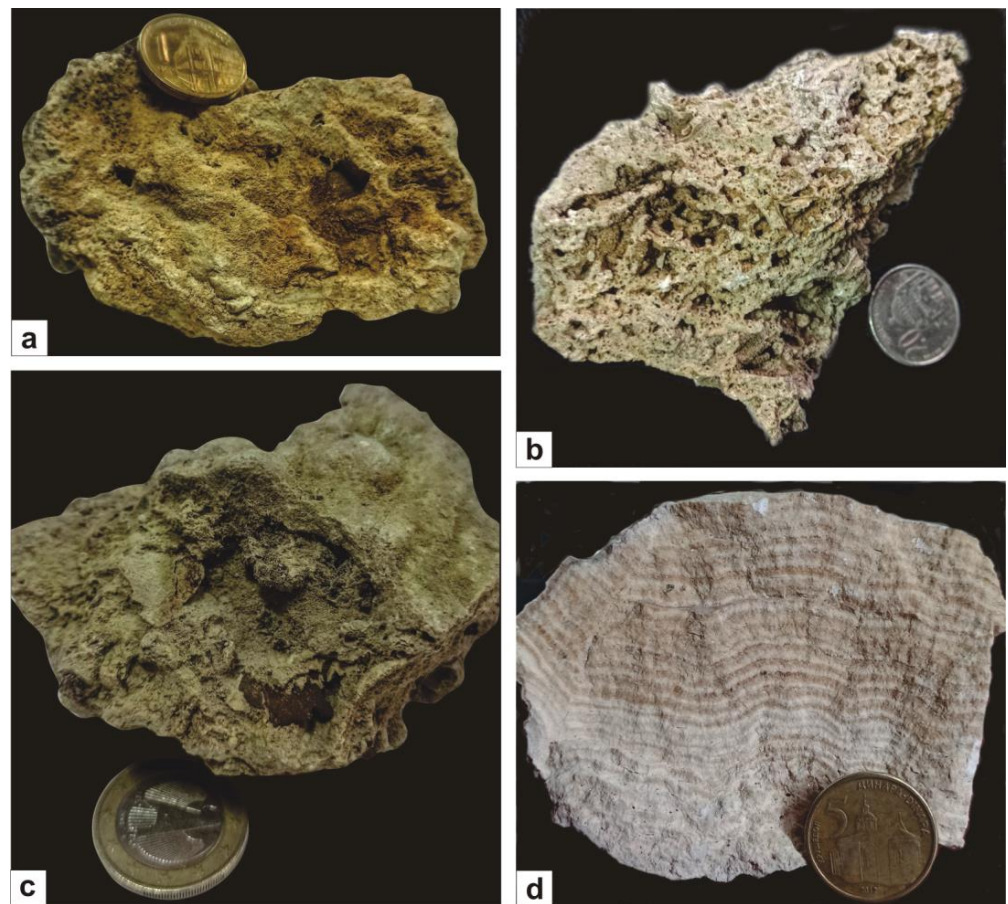
Figure 3. Samples of the most representative tufa samples. (**a**) Algal tufa; (**b**) Moss tufa; (**c**) Phytoclastic tufa; (**d**) Stromatolitic laminated tufa.
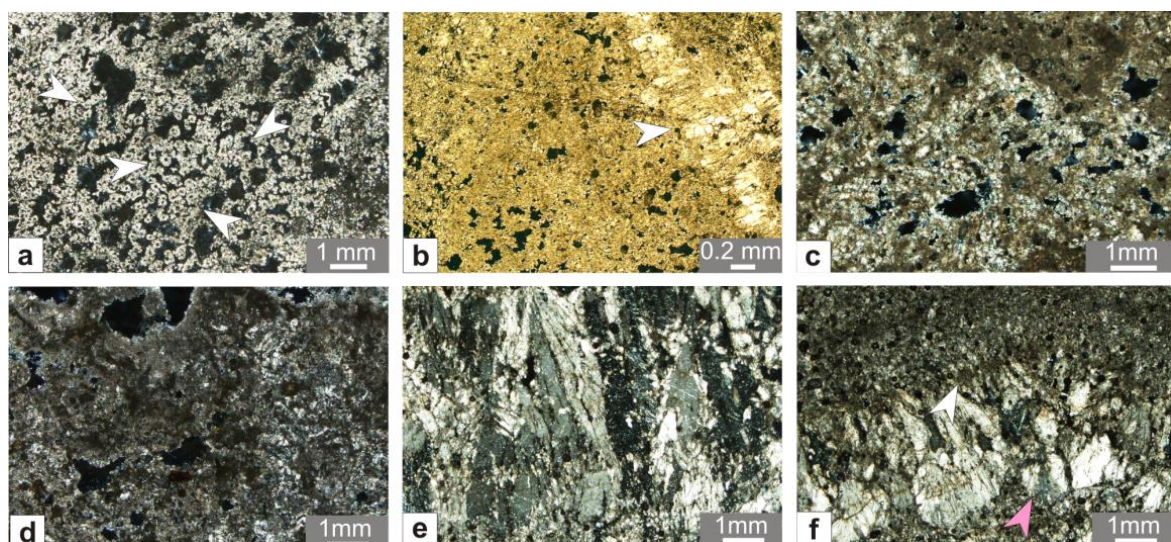

Figure 4. Optical photomicrographs of thin sections. (**a**) Algal tufa. Note regular oval-shaped voids, surrounded by spherical calcite crystals (white arrows); (**b**) Algal tufa. White arrow points to void, filled by sparry calcite crystal; (**c**) Moss tufa built by micrite and sparite; (**d**) Phytoclastic tufa dominantly built by micrite; (**e**) Fan-shaped sparry calcite crystals in stromatolitic laminated tufa; (**f**) Micritic laminae (white arrow) alternates with sparitic laminae (pink arrow) in stromatolitic laminated tufa.
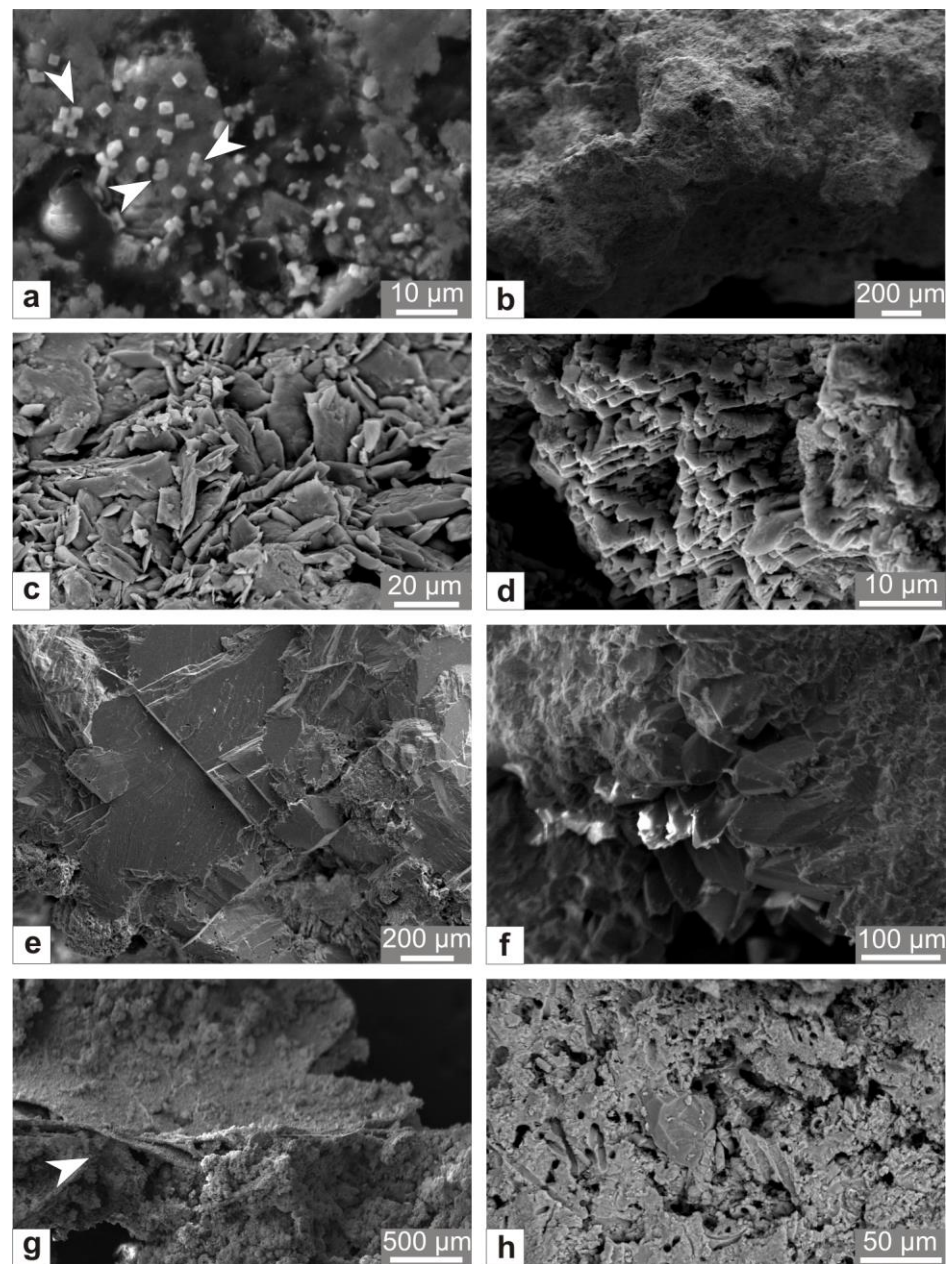
Figure 5. SEM images of tufa samples. (**a**) White arrows point to sylvite crystals; (**b**) Massive calcite aggregate in algal tufa; (**c**) Crystals of a primitive rhombohedron in moss tufa; (**d**) Dagger-like calcite crystals in moss tufa; (**e**) Massive calcite aggregate with well-developed cleavage; (**f**) Scalenohedron calcite crystals; (**g**) Phytoclastic tufa. Note the leaf imprint (white arrow); (**h**) Tubular cavities in calcite left by loss of bacterial filaments.

Algal tufa is usually found at the river bottom, which is intensively occupied by algae (Figure 2i). At some places, it occurs as a thin crust above the host rock. Algal tufa is brownish and, usually, very porous and friable (Figure 3a). It is dominantly built by clotted micrite, with scarce traces of sparite and microsparite, which locally surround micritic grains, forming a rim. Secondary sparry calcite crystals are usually found inside voids of different thicknesses (Figure 4b). Calcite grains are about 0.1 mm in size, and, in this facies, they are generally equal in size and shape. Regular oval-shaped voids are commonly present, surrounded by spherical calcite crystals (Figure 4a). It is observed that algal tufa usually displays massive or clotted textures and does not contain well-developed crystals (Figure 5b).

Stromatolitic laminated tufa is exclusively fossil tufa, usually found in a lower altitude. Stromatolitic laminated tufa is non-porous, very compact, and consists of about 1.5 mm thick light sparitic and dark micritic laminas (Figures 3d and 4f). Usually, light and dark laminas are of equal thickness, but some variations were noted. Respectively, sporadically light sparitic laminas are thicker than the micritic ones. Lamination is horizontal or wavy. In these facies, columnar and fan-shaped or needle-shaped sparite crystals are found in laminas (Figure 4e). Calcite crystals are perpendicular to lamination and occasionally reach 1 mm in length. SEM analyses showed that stromatolitic laminated tufa consists of coarse scalenohedron calcite crystals (Figure 5f) with well-developed cleavage (Figure 5e).

Phytoclastic tufa is formed among the whole river flow, especially at the barrages and small dams. It is more friable and more porous than other facies. These facies contain allochtonous plant fragments, such as leaves and twigs (Figures 3c and 5g). Phytoclastic tufa is almost completely built by clotted micrite, which surrounds numerous irregular and elongated fissures (Figure 4d). The size of the individual crystals is about 5μ. Rarely, secondary calcite crystals are found inside voids. Investigation in scanning electron microscope showed that there are also nanoscopic-sized holes, equal in shape and size, considering the loss of bacterial filaments (Figure 5h).

SEM analysis confirmed the presence of sylvite in two tufa samples from GRB. In one of those samples, sylvite occurs as dendritic aggregates while sylvite crystals appeared in a form of hexahedron in the other cubic (isometric) (Figure 5a). Sylvite crystals are of small dimensions that are usually about 2 μm, with a maximum of up to 3 μm.

4.3. Stable Isotope Composition

Both recent and fossil tufa deposits show similar and relative values of $\delta^{18}O$ and $\delta^{13}C$. The $\delta^{18}O$ values are between $-9.07‰$ and $-10.79‰$ (mean value: $-9.81‰$),whereas $\delta^{13}C$ values range between $-6.50‰$ and $-10.34‰$ (mean values $-9.01‰$). The highest values of $\delta^{18}O$ display fossil tufas from GRB, while the lowest values were recorded in fossil tufa from SRB. The highest values of $\delta^{13}C$ display fossil tufa from SRB, while the lowest values of $\delta^{13}C$ are represented by fossil tufa from GRB. There were no significant differences in the stable isotope composition between the different types and facies of analyzed tufa samples, except Sample Five, which has a significantly higher $\delta^{13}C$ value than the other tufa samples. The results of stable isotope analyses are given in Table 1.

Table 1. Stable isotope values in different tufa facies.

Sample	Site	Facies	$\delta^{18}O$ (‰ VPDB)	$\delta^{13}C$ (‰ VPDB)	Recent vs. Fossil Tufa
1	GRB	Algal tufa	-9.27 ± 0.05	-9.98 ± 0.04	Recent tufa
2	GRB	Phytoclastic tufa	-9.30 ± 0.08	-9.69 ± 0.02	Recent tufa
3	GRB	Stromatolitic laminated tufa	-9.07 ± 0.03	-8.84 ± 0.04	Fossil tufa
4	GRB	Moss tufa	-9.49 ± 0.02	-10.34 ± 0.02	Fossil tufa
5	SRB	Moss tufa	-9.48 ± 0.05	-6.50 ± 0.07	Fossil tufa
6	SRB	Algal tufa	-10.66 ± 0.09	-8.63 ± 0.03	Recent tufa
7	SRB	Stromatolitic laminated tufa	-10.79 ± 0.03	-8.53 ± 0.03	Fossil tufa
8	SRB	Phytoclastic tufa	-10.44 ± 0.01	-9.59 ± 0.02	Recent tufa

5. Discussion

The differences between tufa samples were obvious even macroscopically, especially between recent and fossil tufa samples, as well as evident different facies. Differences between tufa morphologies were influenced by "micro" variations in local conditions and, thus, by the diversity of the flora. In fact, the morphology of the tufa was controlled by a substrate, over which the spring water flows. The distribution of tufa facies points to a clear relationship between facies and local environmental conditions [44].

Moss tufa was, undoubtedly, the dominant facies at the waterfalls (recent tufa), but also in the fossil tufa samples. Algal tufa was mostly found in calmer conditions, such as river bottoms, i.e., recent tufas. Phytoclastic tufas are also recent but were mostly

found among the whole river flow, especially at the barrages. Finally, the least present facies was stromatolitic tufa, and all of those tufa samples were considered fossil ones. In general, moss tufa was dominantly found in high energy conditions, whereas algal tufa and phytoclastic tufa were found in lower energy environments. The biggest difference between fossil and recent samples was that fossil tufa samples were harder and more compact than recent ones. This was expected, because the diagenesis of the tufa also included changes in the primary structural and textural characteristics of it, leading to more compact tufa by filling primary voids [7]. Additionally, the abundance of sparite/micrite, as well as porosity, varied in different facies, as could be seen in provided results.

The appearance of sylvite in two tufa samples was unusual, thus, it requires some explanation. As sylvite is the evaporite mineral that precipitates among the last ones out of solution, it is only found in a very dry saline areas. Nevertheless, supersaturation of certain ions results in salt crystallization, which is also assisted by higher porosity. It is well-known that sylvite is mostly used as a raw material for the production of fertilizers [45]. Thus, we assume that sylvite is most probably the result of anthropogenic contamination.

Origin of Tufa Deposits

Freshwater carbonates such as tufa can be useful tools for environmental conditions, assuming isotopic equilibrium during calcite precipitation. However, equilibrium between water and precipitated calcite is often disturbed due to different factors.

The changes in water temperature are the most responsible for the variations in $\delta^{18}O$. Increasing water temperature is related to decreasing $\delta^{18}O$ values [3]. Thus, we can assume that differences in $\delta^{18}O$ can be related to seasonal changes. Generally, oxygen isotopic composition suggests that tufa precipitated from cold, freshwaters enriched in calcium bicarbonate. Carbon isotope composition suggests that CO_2 is dominantly of an atmospheric origin, with various amounts of soil (organic) CO_2. Sample Five displays a very high carbon isotope value ($-6.50‰$). The carbon isotopes of carbonate rocks seem to be more complex than oxygen isotopes, which may have resulted from the many potential agents (e.g., abiotic and photosynthetic), degassing of CO_2, deposition of calcite, and CO_2 exchange with the atmosphere [46]. A higher $\delta^{13}C$ value in this sample can point to the input of heavier carbon isotope from dissolved limestones.

In general, no attention is paid to stable isotope analyses in tufas in Serbia. Nevertheless, tufa deposits have been studied worldwide as their isotopic composition can point to environmental conditions. A number of studies dealt with tufa deposits from an environmental point of view in the Mediterranean region [17,22,26,39,42,47–52], Central Europe [21,38,53], and Great Britain [54–56]. Stable isotope data of the studied sites were compared with some well-known tufa deposits in Europe at Figure 6.

It is evident that most of the tufa deposits have $\delta^{18}O$ values between $-9.5‰$ and $-6‰$. The highest $\delta^{18}O$ values are recorded in France [42], as well as in Great Britain [54]. It is interesting that stable oxygen values from SRB and GRB are generally lower than in mentioned studies. The most similar $\delta^{18}O$ signatures to SRB and GRB have tufa deposits from Turkey [50], Poland [38], and a part of tufa from Dinaric Karst [17,22], but they are, still, generally higher than tufa from SRB and GRB.

The situation with the $\delta^{13}C$ isotope data is even more complicated, i.e., more variations in different studies are noted. Most of the tufa deposits have $\delta^{13}C$ values between $-10‰$ and $-6‰$. Tufa samples from Serbia display more similarity with other deposits in $\delta^{13}C$ values than in $\delta^{18}O$ values. However, $\delta^{13}C$ values in this study are generally lower than in other sites in Europe. In many studies, $\delta^{13}C$ values in some samples are very high, usually near 0, or even positive [39,47,49,50]. Only data from France [42], and a part of data from Great Britain [54] have lower $\delta^{13}C$ (minimum $-12.1‰$) than the samples from SRB and GRB.
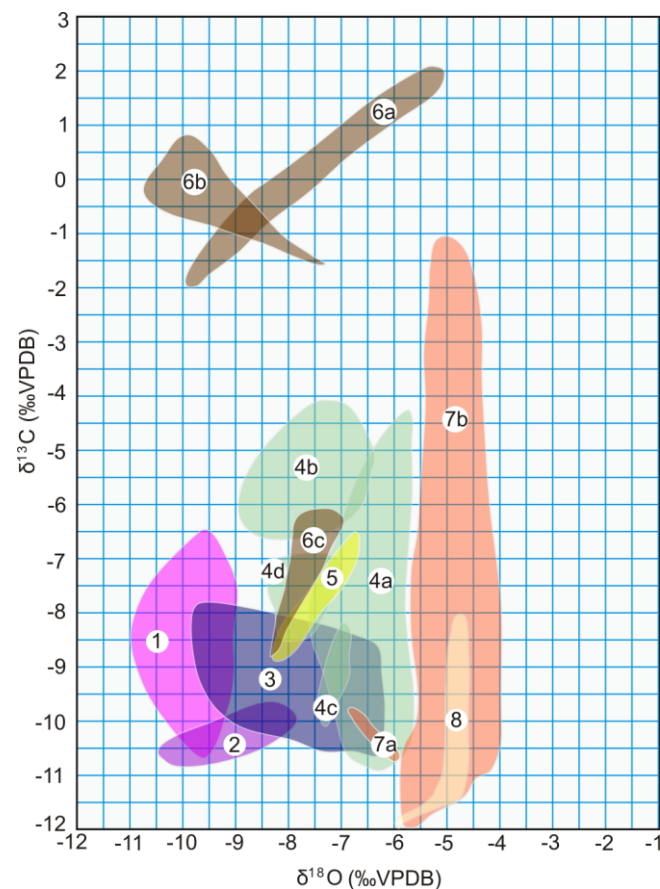
Figure 6. Comparison of stable isotope data in this study with other deposits in Europe. 1. Serbia, present study; 2. Poland [38]; 3. Dinaric Karst [17,22]; 4. Spain: a [47], b [39], c [48], d [51]; 5. Slovakia [53]; 6. Turkey: a [49], b [50], c [52]; 7. Britain: a [55], b [54]; 8. France [42].

Compared to stable isotope analyses of tufa in Dinaric Karst [17,20,22,26], tufa from SRB and GRB have similar δ^{13}C values and lower δ^{18}O values to other tufa accumulations in the region. The comparison between the stable isotope compositions from GRB and SRB to other tufa sites in Dinaric Karst is given in Figure 7. Mean δ^{13}C values for SRB and GRB are −9.01‰, whereas the mean value is −9.60‰ in the Zrmanja River Canyon, Krka River, and Krupa River [17,22,26]. In the Plitvice lakes, mean δ^{13}C values are around −8.1‰ [17]. On the other side, δ^{18}O values are a bit lower for SRB and GRB than in other tufa sites in the region. Mean δ^{18}O values for SRB and GRB is −9.81‰, whereas it is −7.02‰ in the Zrmanja River Canyon [22], −8.08‰ in the Krka River [26], and −7.8‰ in the Krupa River [17]. The most similar to this study are the δ^{18}O values for the Plitvice lakes—with a mean value of −9.7‰ [17].

Generally, δ^{13}C values in tufas from Serbia are lower, but still very similar with the compared regions in Europe. In contrast, the slight differences in the δ^{18}O values suggest that the analyzed tufas could have been formed in slightly different weather or climatic conditions. Most probably, lower values of δ^{18}O relative to other sites in Europe reflect differences in water temperature during tufa crystallization, which is commonly observed in tufas in this part of Europe [57]. Additionally, lower values of δ^{18}O can be caused by the altitude or continental effect on isotopic fractionation in the rainwater that supplies springs, within which tufas are formed [12,58,59]. SRB and GRB are both at higher elevations than the above-mentioned localities (SRB is at 1100 m.a.s.l. and GRB is at 867 m.a.s.l.), whereas the altitude of other sites is usually less than 500 m.a.s.l. According to the observations of [60], the differences in δ^{13}C and δ^{18}O values between analyzed tufa and other sites in the Dinaric region and Europe may result from seasonal differences in

seasonal atmospheric precipitation rates and the degrees of CO_2 degassing along the course of the stream. Comparing only the samples from this study, values are, in general, very similar. Furthermore, the CO_2 source did not change, being mostly atmospheric, and the water temperature was similar all the time during tufa precipitation.
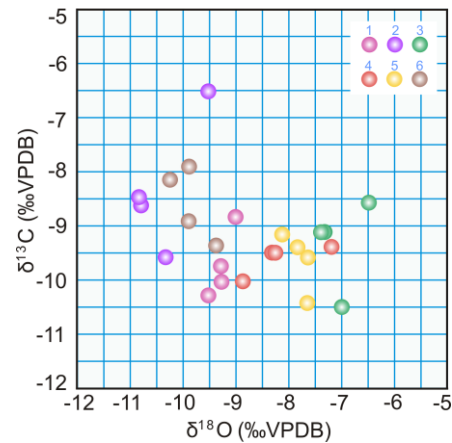

Figure 7. Comparison of stable isotope data in this study with other deposits in Dinaric Karst. 1−Gostilje River Basin; 2−Sopotnica River Basin; 3−Zrmanja River Basin; 4−Krka River Basin; 5−Krupa River Basin; 6−Plitvice Lakes.

6. Conclusions

The investigations of tufa accumulations at SRB and GRB led to the following conclusions:

(1) Four tufa facies are recognized, ordered by their abundance: moss tufa, phytoclastic tufa, algal tufa, and stromatolitic laminated tufa. Different facies display different environmental conditions.

(2) Stable isotope ($\delta^{13}C$ and $\delta^{18}O$) data from the tufa of SRB and GRB are similar in all tufa facies. Oxygen isotope composition suggests that the tufa precipitated from cold, freshwaters enriched in calcium bicarbonate. Carbon isotope composition suggests that CO_2 is dominantly of atmospheric origin, with various amount of soil (organic) CO_2.

(3) Differences in the $\delta^{13}C$ values between the tufa samples from Serbia and from the other sites in Europe are negligible. Lower $\delta^{18}O$ values in the tufa from SRB and GRB than in other sites in Europe indicate that these tufa deposits in Serbia precipitated in a slightly different condition. Lower $\delta^{13}C$ values in tufa from SRB and GRB than in other sites in Europe indicate that in tufa from Serbia, while the influence of isotopically heavier ^{13}C from dissolved limestones was less.

(4) Well-developed sylvite crystals in two samples from GRB suggest a strong anthropogenic influence.

Author Contributions: Conceptualization, N.B.; Methodology, N.B. and V.G.; Software, U.D. and A.V.; Investigation, V.G.; Data curation, I.C. and V.G.; Writing—review & editing, N.B. and I.C.; Visualization, N.B., W.W., I.C. and U.D.; Supervision, W.W. All authors have read and agreed to the published version of the manuscript.

Institutional Review Board Statement: Not applicable.

Informed Consent Statement: Not applicable.

Data Availability Statement: The data presented in this study are available on request from the corresponding author.

Conflicts of Interest: The authors declare no conflict of interest.

References

1. Roche, A.; Vennin, E.; Bundeleva, I.; Bouton, A.; Payandi-Rolland, D.; Amiotte-Suchet, P.; Gaucher, E.C.; Courvoisier, H.; Visscher, P.T. The Role of the Substrate on the Mineralization Potential of Microbial Mats in a Modern Freshwater River (Paris Basin, France). *Minerals* **2019**, *9*, 359. [CrossRef]
2. Gandin, A.; Capezzuoli, E. Travertine vs. calcareous tufa: Distinctive petrologic features and stable isotope signatures. *Ital. J. Quat. Sci.* **2008**, *21*, 125–136.
3. Andrews, J.E. Palaeoclimatic records from stable isotopes in riverine tufas: Synthesis and review. *Earth Sci. Rev.* **2006**, *75*, 85–104. [CrossRef]
4. Hamdan, M.A.; Brook, G.A. Timing and characteristics of Late Pleistocene and Holocene wetter periods in the Eastern Desert and Sinai of Egypt, based on ^{14}C dating and stable isotope analysis of spring tufa deposits. *Quat. Sci. Rev.* **2015**, *130*, 168–188. [CrossRef]
5. Brogi, A.; Capezzuoli, E.; Buracchi, E.; Branca, M. Tectonic control on travertine and calcareous tufa deposition in a low-temperature geothermal system (Sarteano, Central Italy). *J. Geol. Soc. Lond.* **2012**, *169*, 461–476. [CrossRef]
6. Capezzuoli, E.; Gandin, A.; Pedley, M. Decoding tufa and travertine (fresh water carbonates) in the sedimentary record: The state of the art. *Sedimentology* **2014**, *61*, 1–21. [CrossRef]
7. Ford, T.D.; Pedley, H.M. A review of tufa and travertine deposits of the world. *Earth Sci. Rev.* **1996**, *41*, 117–175. [CrossRef]
8. Liu, L. Factors Affecting Tufa Degradation in Jiuzhaigou National Nature Reserve, Sichuan, China. *Water* **2017**, *9*, 702. [CrossRef]
9. Đurović, P. *Bigar—Značajna prirodna vrednost krasa u Srbiji, Zaštita prirode [Tufa—significant natural value of Serbian karst. Nature conservation]*; Zavod za zaštitu prirode: Beograd, Srbije, 1998; pp. 163–170.
10. Sancho, C.; Arenas, C.; Vázquez-Urbez, M.; Pardo, G.; Lozano, V.M.; Peña-Monné, L.J.; Hellstrom, C.J.; Ortiz, E.J.; Osácar, C.M.; Auqué, L.; et al. Climatic implications of the Quaternary fluvial tufa record in the NE Iberian Peninsula over the last 500 ka. *Quat. Res.* **2015**, *84*, 398–414. [CrossRef]
11. Andrews, J.E.; Riding, R.; Dennis, F.P. The stable isotope record of environmental and climatic signals in modern terrestrial microbial carbonates from Europe. *Palaeogeogr. Palaeoclimatol. Palaeoecol.* **1997**, *129*, 171–189. [CrossRef]
12. Andrews, J.E.; Pedley, M.; Dennis, F.P. Palaeoenvironmental records in Holocene Spanish tufas: A stable isotope approach in search of reliable climatic archives. *Sedimentology* **2000**, *47*, 961–978. [CrossRef]
13. Brook, G.A.; Cherkinsky, A.; Railsback, L.B.; Marais, E.; Hipondoka, M.H.T. ^{14}C dating of organic residue and carbonate from stromatolites in Etosha Pan. Namibia: ^{14}C reservoir effect: Correction of published ages and evidence of >8-m-deep lake during the late Pleistocene. *Radiocarbon* **2013**, *55*, 1156–1163. [CrossRef]
14. Domínguez-Villar, D.; Vázquez-Navarro, J.A.; Cheng, H.; Edwards, R.L. Freshwater tufa record from Spain supports evidence for the past interglacial being wetter than the Holocene in the Mediterranean region. *Glob. Planet. Chang.* **2011**, *77*, 129–141. [CrossRef]
15. Dabkowski, J. The late-Holocene tufa decline in Europe: Myth or reality? *Quat. Sci. Rev.* **2020**, *230*, 106141. [CrossRef]
16. Hasan, O.; Miko, S.; Brunović, D.; Papatheodorou, G.; Christodolou, D.; Ilijanić, N.; Geraga, M. Geomorphology of Canyon Outlets in Zrmanja River Estuary and Its Effect on the Holocene Flooding of Semi-enclosed Basins (the Novigrad and Karin Seas, Eastern Adriatic). *Water* **2020**, *12*, 2807. [CrossRef]
17. Horvatinčić, N.; KrajcarBronić, I.; Obelić, B. Diferences in the ^{14}C age, δ^{13}C and δ^{18}O of Holocene tufa and speleothem in the Dinaric Karst. *Palaeogeogr. Palaeoclimatol. Palaeoecol.* **2003**, *193*, 139–157. [CrossRef]
18. Pentecost, A. *Travertine*; Springer: Berlin/Heidelberg, Germany, 2005; p. 445.
19. Sherriff, J.E.; Schreve, D.C.; Candy, I.; Palmer, A.P.; White, T.S. Environments of the climatic optimum of MIS 11 in Britain:Evidence from the tufa sequence at Hitchin, southeast England. *J. Quat. Sci.* **2021**, *36*, 508–525. [CrossRef]
20. Zavadlav, S.; Rožič, B.; Dolenec, M.; Lojen, S. Stable isotopic and elemental characteristics of recent tufa from a karstic Krka River (south-east Slovenia): Useful environmental proxies? *Sedimentology* **2016**, *64*, 808–831. [CrossRef]
21. Gruszczyński, T.; Małecki, J.J.; Romanova, A.; Ziułkiewicz, M. Reconstruction of Thermal Conditions in the Subboreal Inferred from Isotopic Studies of Groundwater and Calcareous Tufa from the Spring Mire Cupola in Wardzyń (Central Poland). *Water* **2019**, *11*, 1945. [CrossRef]
22. Barešić, J.; Faivre, S.; Sironić, A.; Borković, D.; Lovrenčić Mikelić, I.; Drysdale, R.N.; Krajcar Bronić, I. The Potential of Tufa as a Tool for Paleoenvironmental Research—A Study of Tufa from the Zrmanja River Canyon, Croatia. *Geosciences* **2021**, *11*, 376. [CrossRef]
23. Horvatinčić, N.; Ćalić, R.; Geyh, M.A. Interglacial Growth of Tufa in Croatia. *Quat. Res.* **2000**, *53*, 185–195. [CrossRef]
24. Lojen, S.; Dolenec, T.; Vokal, B.; Cukrov, N.; Mihelčić, G.; Papesch, W. C and O stable isotope variability in recent freshwater carbonates (River Krka, Croatia). *Sedimentology* **2004**, *51*, 361–375. [CrossRef]
25. Lojen, S.; Trkov, A.; Ščančar, J.; Vázquez-Navarro, J.A.; Cukrov, N. Continuous 60-year stable isotopic and earth-alkali element records in a modern laminated tufa (Jaruga, river Krka, Croatia): Implications for climate reconstruction. *Chem. Geol.* **2009**, *258*, 242–250. [CrossRef]
26. Rovan, L.; Zuliani, T.; Horvat, B.; Kanduč, T.; Vreča, P.; Jamil, Q.; Čermelj, B.; Bura-Nakić, E.; Cukrov, N.; Štrok, M.; et al. Uranium isotopes as a possible tracer of terrestrial authigenic carbonate. *Sci. Total Environ.* **2021**, *797*, 149103. [CrossRef] [PubMed]

27. Srdoč, D.; Horvatincic, N.; Obelic, B.; Krajcar, I.; Sliepcevic, A. Procesi taloženja kalcita u krškim vodama s posebnim osvrtom na Plitvicka jezera (Calcite deposition processes in karst waters with special emphasis on the Plitvice Lakes, Yugoslavia). *KRS Jugosl.* **1985**, *11*, 1–104.

28. Horvatinčić, N.; Barešić, J.; Babinka, S.; Obelić, B.; Krajcar Bronić, I.; Vreča, P.; Suckow, A. Towards a deeper understanding how carbonate isotopes (^{14}C, ^{13}C, ^{18}O) reflect environmental changes: A study with recent ^{210}Pb dated sediments of the Plitvice lakes, Croatia. *Radiocarbon* **2008**, *50*, 233–253. [CrossRef]

29. Srdoč, D.; Obelić, B.; Horvatinčić, N. Radiocarbon dating of calcareous tufa: How reliable data can we expect? *Radiocarbon* **1980**, *22*, 858–862. [CrossRef]

30. Srdoč, D.; Krajcar Bronić, I. The application of stable and radioactive isotopes in karst water research. *NašKrš* **1986**, *12*, 37–47.

31. Karamata, S. The geodynamic framework of the Balkan Peninsula: Its origin due to the approach, collision and compression of Gondwanian and Eurasian units. In *Tectonic Development of the Eastern Mediterranean Region*; Robertson, A.H.F., Mountrakis, D., Eds.; Geological Society: London, UK, 2006; Volume 260, pp. 155–178.

32. Robertson, A.; Karamata, S.; Šarić, K. Overview of ophiolites and related units in the Late Paleozoic—Early Cenozoic magmatic and tectonic development of Tethys in the northern part of the Balkan region. *Lithos* **2009**, *108*, 1–36. [CrossRef]

33. Gavrilović, D. *The Karst of Serbia*; Memories of the Serbian Geographical Society 13: Belgrade, Serbia, 1976; pp. 1–28.

34. Kranjc, A. Dinaric Karst. In *Encyclopedia of Caves and Karst Science*; Gunn, J., Ed.; Fitzroy Dearborn: New York, NY, USA; London, UK, 2004; pp. 287–289.

35. Milivojević, M. Hydrogeothermal system of Zlatibor. In *Geologija Zlatibora (Geology of Zlatibor)*; Dimitrijević, M.D., Ed.; Geoinistitut: Beograd, Srbija, 1996; Volume 18, pp. 121–130.

36. Oliveira, E.C.; Rossetti, D.F.; Utida, G. Paleoenvironmental Evolution of Continental Carbonates in West-Central Brazil. *An. Acad. Bras. Ciênc.* **2017**, *89*. [CrossRef]

37. Andrews, J.E.; Brasier, A.T. Seasonal records of climatic change in annually laminated tufas: Short review and future prospects. *J. Quat. Sci.* **2005**, *20*, 411–421. [CrossRef]

38. Pazdur, A.; Pazdur, M.F. Stable isotopes of Holocene calcareous tufa in southern Poland as paleoclimatic indicators. *Quat. Res.* **1988**, *30*, 177–189. [CrossRef]

39. Soriano, M.C.O.; Abad, C.A.; Marcén, C.A.; Tirapu, G.P.; Bello, L.M. Stable-isotope changes in tufa stromatolites of the Quaternary Añamaza fluvial system (Iberian Ranges, Spain). *Geogaceta* **2017**, *61*, 167–170.

40. Pedley, H.M. Tufas and travertines of the Mediterranean region: A testing ground for freshwater carbonate concepts and developments. *Sedimentology* **2009**, *56*, 221–246. [CrossRef]

41. Martín-Algarra, A.; Martín-Martín, M.; Andreo, B.; Juliá, R.; González-Gómez, C. Sedimentary patterns in perched spring travertines near Granada (Spain) as indicators of the paleohydrological and paleoclimatological evolution of a karst massif. *Sediment Geol.* **2003**, *161*, 217–228. [CrossRef]

42. Dabkowski, J.; Limondin-Lotouet, N.; Antoine, P.; Andrews, J.E.; Marca-Bell, A.; Robert, V. Climatic variations in MIS 11 recorded by stable isotopes and trace elements in a French tufa (La Celle, Seine Valley). *J. Quatern. Sci.* **2012**, *27*, 790–799. [CrossRef]

43. Beisel, R.H., Jr. *International Waterfall Classification System*; Outskirts Press: Parker, CO, USA, 2006; p. 294.

44. Gradzinski, M. Factors controlling growth of modern tufa: Results of a field experiment. In *Tufas and Speleothems*; Pedley, H.M., Rogerson, M., Eds.; Geological Society of London: London, UK, 2010; Volume 336, pp. 143–191. [CrossRef]

45. Castro-Suarez, J.R.; Colpas-Castillo, F.; Taron-Dunoyer, A. Chemical and Morphologic Characterization of Sylvite (KCl) Mineral from Different Deposits Used in the Production of Fertilizers. *Agronomy* **2023**, *13*, 52. [CrossRef]

46. Matsuoka, J.; Kano, A.; Oba, T.; Watanabe, T.; Sakai, S.; Seto, K. Seasonal variation of stable isotopic compositions recorded in a laminated tufa, SW Japan. *Earth Planet. Sci. Lett.* **2001**, *192*, 31–44. [CrossRef]

47. Ortiz, J.E.; Torres, T.; Delgado, A.; Reyes, E.; Diaz-Bautista, A. A review of the Tagus river tufa deposits (central Spain): Age and palaeoenvironmental record. *Quat. Sci. Rev.* **2009**, *28*, 947–963. [CrossRef]

48. Melon, P.; Alonso-Zarza, A.M. The Villaviciosa tufa: A scale model for an active cool water tufa system, Guadalajara (Spain). *Facies* **2018**, *64*, 5. [CrossRef]

49. Kosun, E. Facies characteristics and depositional environments of Quaternary tufa deposits, Antalya, SW Turkey. *Carbonates Evaporites* **2012**, *27*, 269–289. [CrossRef]

50. Toker, E. Quaternary fluvial tufas of Sarıkavak area, southwestern Turkey: Facies and depositional systems. *Quat. Int.* **2017**, *437*, 37–50. [CrossRef]

51. Arenas, C.; Osacar, C.; Sancho, C.; Vasquez-urbez, M.; Auque, L.; Pardo, G. Seasonal record from recent fluvial tufa deposits (Monasterio de Piedra, NE Spain): Sedimentological and stable isotope data. In *Tufas and Speleothems*; Pedley, H.M., Rogerson, M., Eds.; Geological Society of London: London, UK, 2010; Volume 336, pp. 119–142.

52. Ozkul, M.; Gokgoz, A.; Horvatincic, N. Depositional properties and geochemistry of Holocene perched springline tufa deposits and associated spring waters: A case study from the Denizli Province, Western Turkey. In *Tufas and Speleothems*; Pedley, H.M., Rogerson, M., Eds.; Geological Society of London: London, UK, 2010; Volume 336, pp. 245–262.

53. Dabkowski, J.; Frodlova, J.; Hajek, M.; Hajkova, P.; Petr, L.; Fiorillo, D.; Dudova, L.; Horsak, M. A complete Holocene climate and environment record for the Western Carpathians (Slovakia) derived from a tufa deposit. *Holocene* **2018**, *9*, 493–504. [CrossRef]

54. Andrews, J.E.; Riding, R.; Dennis, P.F. Stable isotopic compositions of recent freshwater cyanobacterial carbonates from the British Isles: Local and regional environmental controls. *Sedimentology* **1993**, *40*, 303–314. [CrossRef]

55. Andrews, J.E.; Pedley, H.M.; Dennis, P.F. Stable isotope record of palaeoclimatic change in a British Holocene tufa. *Holocene* **1994**, *4*, 349–355. [CrossRef]

56. Garnett, E.R.; Andrews, J.E.; Preece, R.C.; Dennis, P.F. Climatic change recorded by stable isotopes and trace elements in a British Holocene tufa. *J. Quat. Sci.* **2004**, *19*, 251–262. [CrossRef]

57. Bódai, B.; Czuppon, G.; Fórizs, I.; Kele, S. Seasonal study of calcite-water oxygen isotope fractionation at recent freshwater tufa sites in Hungary. *Geol. Carpathica* **2022**, *73*, 485–496. [CrossRef]

58. Kern, Z.; Hatvani, I.G.; Czuppon, G.; Fórizs, I.; Erdélyi, D.; Kanduč, T.; Palcsu, L.; Vreča, P. Isotopic 'altitude' effect and 'continental' effect in modern precipitation across the Adriatic–Pannonian region. *Water* **2020**, *12*, 1797. [CrossRef]

59. Gonfiantini, R.; Roche, M.; Olivry, J.; Fontes, J.; Zuppi, G. The altitude effect on the isotopic composition of tropical rains. *Chem. Geol.* **2001**, *181*, 147–167. [CrossRef]

60. Hori, M.; Kawai, T.; Matsuoka, J.; Kano, A. Intra-annual perturbations of stable isotopes in tufas: Effects of hydrological processes. *Geochim. Cosmochim. Acta* **2009**, *73*, 1684–1695. [CrossRef]